Available online at www.sciencedirect.com

SciVerse ScienceDirect

Ceramics International 39 (2013) 4321–4328

CERAMICS INTERNATIONAL

www.elsevier.com/locate/ceramint

A versatile route for the preparation of Ni–CGO cermets from nanocomposite powders

Daniel A. Macedo[a,*], Graziele L. Souza[b], Beatriz Cela[c], Carlos A. Paskocimas[a], Antonio E. Martinelli[a], Filipe M.L. Figueiredo[d], Fernando M.B. Marques[d], Rubens M. Nascimento[a,*]

[a]*Materials Science and Engineering Postgraduate Program, UFRN, Natal 59072-970, Brazil*
[b]*Department of Chemical Engineering, UFRN, Natal 59072-970, Brazil*
[c]*Forschungszentrum Jülich GmbH, ZAT, Jülich, Germany*
[d]*Department of Materials and Ceramic Engineering, University of Aveiro, 3810-193 Aveiro, Portugal*

Received 24 September 2012; received in revised form 5 November 2012; accepted 6 November 2012
Available online 14 November 2012

Abstract

A comparative microstructural study between Ni–$Ce_{0.9}Gd_{0.1}O_{1.95}$ (Ni–CGO) anodes obtained from NiO–CGO nanocomposite powders prepared by in situ one-step synthesis and by mechanical mixture (two-step synthesis) of NiO and CGO powders is reported. The open porosity and microstructure of sintered and reduced pellets were investigated as a function of the citric acid content used as pore forming agent. Nanosized crystallites for the one-step and two-step routes were around 18 nm and 24 nm against 16 nm and 37 nm, for CGO and NiO, respectively. Overall results show that both routes provided suitable microstructures either for anode-support, or for functional anodes for solid oxide fuel cells (SOFCs), with more versatile characteristics in the case of the one-step route. The electrical characterization of selected NiO–CGO samples, carried out between 90 and 260 °C by impedance spectroscopy, confirms electrical percolation of both phases in the composites. However, based on combined microstructural and impedance data, it seems clear that the one-step processing route is the best approach to make SOFC anodes with improved performance.

Keywords: One-step synthesis; Ni–CGO anode; Microstructure; Impedance spectroscopy

1. Introduction

Ni–$Ce_{0.9}Gd_{0.1}O_{1.95}$ (Ni–CGO) ceramic-metal composites (cermets) are widely used as anode materials for the electrochemical oxidation of fuels in solid oxide fuel cells (SOFCs) [1]. In these composite materials, Ni acts as catalyst for fuel oxidation and provides electronic conductivity, whereas CGO mainly acts as a matrix to support the catalyst and to prevent Ni from agglomerating both during sintering and operation. The choice of CGO instead of the traditional yttria stabilized zirconia (YSZ) as the ceramic component in porous cermet anodes results in better matching of thermal expansion coefficients between the anode and CGO as electrolyte [2,3]. Another noticeable advantage of doped ceria based anodes is related to their exceptional tolerance to high sulfur levels in the fuel, which is probably the result of a stronger chemical affinity between CeO_2 and S than between Ni and S [4].

The electrocatalytic activity of these electrodes towards fuel oxidation is known to be critically related to the triple phase boundary (TPB) line, where fuel (e.g., natural gas, biogas, hydrogen, or other H_2 rich gases), electronic (Ni) and ionic conductor (CGO) meet together. The electrode reaction region, along the TPB length, which determines the performance of a Ni–CGO anode, is critically dependent on the microstructure, especially on grain size, porosity, surface area, tortuosity and connectivity [1–3]. Since ceria-based solid electrolytes show significant electronic conductivity under reducing conditions, this means that the active anodic reaction zone may be slightly

*Corresponding authors. Tel.: +55 84 3215 3826; fax: +55 84 3215 3183.
E-mail addresses: damaced@gmail.com (D.A. Macedo), rmaribondo@ufrnet.br (R.M. Nascimento).

0272-8842/$ - see front matter © 2012 Elsevier Ltd and Techna Group S.r.l. All rights reserved.
http://dx.doi.org/10.1016/j.ceramint.2012.11.014

extended along the ceramic phase in the vicinity of the TPB line. Irrespective of this, the length of the TPB is essential in determining this active electrode reaction zone.

It is well established that fine Ni and oxide ion conducting ceramic particles yield better electrical and electrochemical anodic performance when compared to coarse particles [5–7]. This is commonly associated with a high density of Ni-to-CGO contacts, which provide a well-connected network in the anode microstructure, increasing the TPB length and hence also the electrochemical performance [8,9].

It is also well established that the performance and microstructural characteristics of functional materials for SOFC applications are strongly dependent on the powder preparation method. Ni–CGO cermet anodes are usually prepared by mechanical mixing of NiO and CGO powders, subsequently sintered and reduced. The NiO reduction is normally carried out in situ either before or during the first cell start-up run. Despite being simple and allowing accurate compositional control, this conventional method strongly depends on the characteristics of the starting powders and processing route. As a result, the distribution of elements is often non-uniform, yielding inhomogeneous microstructures and poor anode performance [10–13].

Coarsening of Ni grains due to sintering is a major problem as it leads to a reduction of the TPB length and concomitant loss in performance. This problem may be hampered by using cermet nanopowders with fine and homogeneous distribution of the Ni particles within the ceramic matrix. The reported attempts to obtain powders with such characteristics are numerous, including the hydroxide co-precipitation of NiO–$Ce_{0.9}Gd_{0.1}O_{1.95}$ [11], the synthesis by combustion of Ni–YSZ [14], Ni–$CaZr_{0.95}Y_{0.05}O_{2.975}$ and Ni–$SrZr_{0.95}Y_{0.05}O_{2.975}$ [15], the polymeric organic complex solution method in aqueous media to prepare Ni–CGO [16], and the buffer-solution method to synthesize NiO/YSZ [17]. We have recently reported a novel low cost method to prepare Ni–CGO cermets with extended TPB length and enhanced electrochemical performance. These cermets result from the reduction of NiO–CGO nanocomposite powders obtained by a one-step synthesis method, directly from polymeric precursors of both NiO and CGO phases [18].

Besides the nature of the starting composite powders, the incorporation of pore forming materials, which decompose during heat treatment, has been an effective way to design anode microstructures with controlled porosity indicated for easy transport of the reactant and/or product gases. Flour, rice starch, graphite, and a mixture of activated carbon and flour are examples of widely used pore-formers [19–23]. Although these studies have reported the use of pore former agents to produce different anode microstructures, there is no information regarding the influence of the pore former content on the microstructure of Ni–CGO cermet anodes derived from nanocomposite powders.

Although nickel-doped ceria has been widely used as anode material, little information [24,25] is available regarding the electrical properties of the precursor anode material, i.e., NiO–CGO. Here, we return to our one-step synthesis methodology to investigate the effects of the powder synthesis method and the role of a pore forming agent (citric acid) on the microstructure of Ni–CGO cermet anodes. Scanning electron microscopy was used to compare the microstructures of Ni–CGO pellets relative to the amount of added pore former. Electrical properties of selected samples of the anode precursor material (NiO–CGO) were also investigated by impedance spectroscopy aiming at the confirmation of proper percolation of all phases before reduction.

2. Experimental

NiO–$Ce_{0.9}Gd_{0.1}O_{1.95}$ (NiO–CGO) composite powders with 50 wt% CGO and 50 wt% NiO were prepared by two different processes. The first one is the so-called one-step synthesis, a novel sol-gel based method in which resins are obtained from polymeric precursors and then thermally treated to directly produce the NiO–CGO precursor powder [18]. The second approach adopted the conventional mechanical mixture of individual constituents, herein named two-step synthesis. It consists in the separate synthesis of NiO and CGO precursor powders which are then ball milled after calcination at 800 °C for 2 h, to obtain the composite powder. Further details of the preparation of these composite powders were previously described [18]. The nickel oxide content used in this work was 39 vol% Ni (50 wt% NiO, before heat treatment in reducing atmosphere), identified as the adequate amount of Ni for percolation threshold in a nickel based cermet anode [26].

The NiO–CGO composite powders and proper quantities of citric acid as pore former were mixed and ground in an agate mortar. Afterwards, the powders were uniaxially pressed into pellets at 198 MPa and then sintered in air at 1300 °C for 4 h. This is the optimal temperature to obtain the desired porosity avoiding densification, as inferred by dilatometric analysis. The sintered NiO–CGO ceramics were reduced to Ni–CGO cermets by thermal treatment in H_2 (10 vol%, diluted in N_2) at 900 °C for 1 h. The prepared samples are referred to as 1CGONiO-x or 1CGONi-x for the one-step series and 2CGONiO-x or 2CGONi-x for the two-step series, where $x=0$, 5, 10, 15 or 20, corresponds to the wt% of citric acid with respect to the mass of NiO–CGO.

The composite powders as well as the sintered and reduced ceramics were characterized by X-ray diffraction (XRD) using a Shimadzu XRD-7000 diffractometer (CuK_α radiation, with 40 kV and 40 mA). The diffraction patterns were obtained within the angular range of $10 \le 2\theta \le 80^\circ$ in step-scanning mode (0.02°/step, 2 s/step). The lattice parameters were estimated by Rietveld refinement of the XRD data using the DBWS-9870 computer program [27], as described in detail elsewhere [28]. The experimental full width at half maximum (FWHM) was corrected from the instrumental contribution by using the lantanum-hexaborate (LaB_6) standard, and the crystallite size was determined with the Scherrer equation [28]. The open porosity of both sintered and reduced disk-shaped

pellets was measured by the Archimedes method. The microstructure of the Ni–CGO cermets was examined by scanning electron microscopy (SEM) in a Philips ESEM-XL30 microscope. The electrical characterization was carried out by impedance spectroscopy to evaluate the conductivity of selected non-reduced samples. The spectra were collected in air from 90 to 260 °C using one Hewlett Packard 4284A LCR meter. The frequency range was between 20 Hz and 1 MHz with test signal amplitude of 0.5 V. Before the electrical measurements, Pt paste was deposited on both faces of the pellets and porous Pt electrodes were obtained after firing in air at 1000 °C for 1 h.

3. Results and discussion

Fig. 1 shows the XRD patterns of NiO–CGO composite powders (without the addition of citric acid) prepared by one- and two-steps methods after firing at 800 °C for 2 h, together with patterns for the corresponding Ni–CGO cermets obtained after a 1 h treatment in H_2 atmosphere at 900 °C. As expected, there are no peaks from phases other than NiO and CGO in the as synthesized powders, or Ni and CGO in the cermets.

The patterns can be indexed with the expected cubic space groups for CGO (space group Fm-3 m, JCPDS card file n° JCPDS 75-0161), NiO (Fm-3 m, JCPDS card file n° 47-1049) or Ni (Fm-3 m, JCPDS card file n° 04-0850) for Rietveld refinement. The obtained fitting parameters are presented in Table 1, including the lattice parameter, the crystallite size and the weight fraction of each phase. The agreement factors R_{wp} and R_{exp} of the Rietveld analysis are also listed in Table 1. These values, particularly R_{wp}, are higher for the reduced materials due to the difficulty of fitting the profile shapes. Nevertheless, the obtained low χ^2 (goodness-of-fit) values indicate a good quality fit. The first thing to note is that the estimated fractions of each phase are in good agreement with the nominal composition

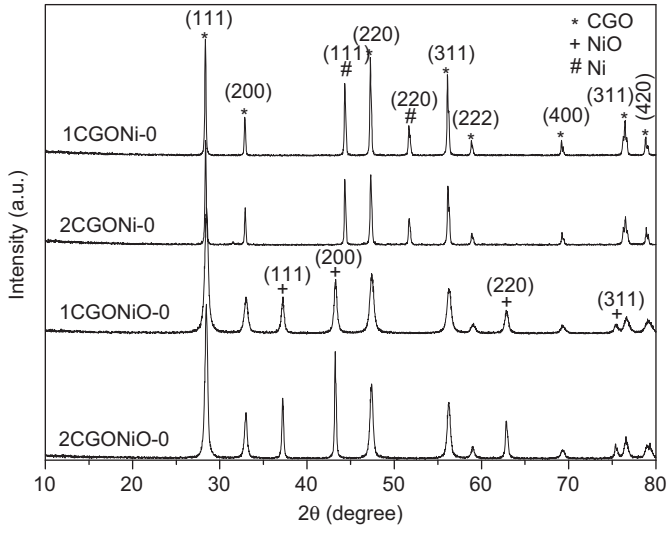

Fig. 1. XRD patterns of NiO–CGO powders and Ni–CGO cermets without citric acid.

(50 wt% NiO and 39 wt% Ni). No substantial differences are seen in the lattice parameters of each phase (CGO and NiO or Ni). Comparing the D_{XRD} values, it is noteworthy that both methods yield very similar size for the CGO (16–18 nm), whereas D_{XRD} for the NiO is smaller in the case of the one-step synthesis. This difference may be due to the intimate mixture of the two phases obtained by the one-step approach, where the number of NiO–NiO contacts is reduced due to intimately dispersed CGO particles. Regardless of the synthesis method, the NiO crystallite size appears as larger than that of CGO, which suggests that NiO crystallites grow faster than those of the CGO phase.

The values of D_{XRD} (16–37 nm) are somewhat lower than those reported in the literature: 27.3 nm (CGO) and 30.5 nm (NiO) for powders synthesized by a hydroxide co-precipitation method [11], 40–50 nm (CGO) and 30–58 nm (NiO) for powders obtained by solution combustion synthesis [24], and 53.7 nm for CGO powders prepared by a citrate complexation method [29], obtained under similar firing conditions.

The XRD diffraction peaks for the reduced samples are clearly sharper than for the corresponding NiO–CGO mixtures, suggesting substantial grain growth during the high temperature reduction. This is expected as a result of the additional heat treatment (at 1300 °C in air plus 900 °C in H_2+N_2) under reducing conditions, leading to the formation of metallic nickel (with enhanced sintering kinetics).

Fig. 2 shows the values of open porosity for sintered (NiO–CGO) and reduced (Ni–CGO) samples as a function of the amount of pore former. The open porosity of all samples increases with the addition of pore forming agent. Much higher values of porosity throughout the concentration range of citric acid were found in the sintered sample derived from one-step nanocomposite powders. This phenomenon can be attributed to the presence of carbonaceous residues in the powders obtained via the chemical route synthesis, as previously reported for the synthesis of NiO–CGO nanocomposite powders by the polymeric organic complex solution method [30]. This represents a key advantage of the one-step synthetic route as it provides additional flexibility of the processing conditions (e.g., sintering temperature) allowing the mechanical consolidation of the electrodes with the highest possible level of porosity.

Obviously, under constrained shrinkage due to the presence of the ceramic skeleton, the oxygen loss associated with the reduction of NiO to Ni leads to a significant enhancement of the porosity of sintered samples, resulting directly from the lower density of NiO (6.808 g/cm^3 according to JCPDS 47-1049) when compared to Ni (8.911 g/cm^3 according to JCPDS 04-0850). This should be taken into account for the attainment of Ni-based anodes with controlled porosity.

It is clear from Fig. 2 that for the one-step cermets under study, only the sample labeled 1CGONi-0 exhibits porosity below 50%. This suggests that one-step powders with the thermal history tested in this work (i.e., sintered at 1300 °C for 4 h followed by NiO reduction at 900 °C for 1 h), do

Table 1
Structural parameters and Rietveld agreement indexes for the composite NiO–CGO powders and Ni–CGO cermets, without citric acid. The data in square brackets are the weight fractions of each phase.

Sample	*CGO (JCPDS 75–0161)*		*NiO (JCPDS 47–1049) or Ni (JCPDS 04–0850)*		*Agreement factors*		
	D_{XRD} (nm)	a (Å)	D_{XRD} (nm)	a (Å)	R_{wp} (%)	R_{exp} (%)	χ^2
1CGONiO-0	18 [49%]	5.4151(6)	24 [51%]	4.1766(5)	14.93	12.04	1.24
2CGONiO-0	16 [48%]	5.4148(5)	37 [52%]	4.1768(6)	15.76	12.26	1.28
1CGONi-0	[57%]	5.417135(7)	[43%]	3.523103(2)	21.71	16.50	1.31
2CGONi-0	[59%]	5.413018(7)	[41%]	3.522857(7)	22.39	17.02	1.31

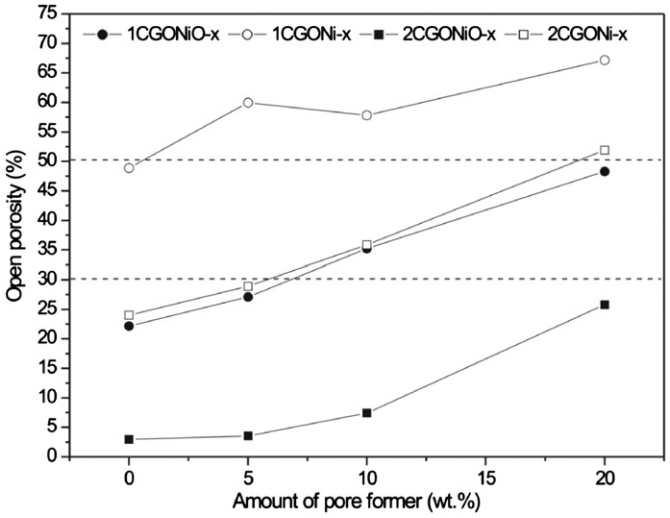

Fig. 2. Open porosity of the sintered and reduced samples as a function of the amount of pore former.

not require pore forming agents. Highly porous Ni-based cermets with porosity levels around 30–40% have been reported [31,32]. Lee et al. [31] investigated the effects of the powder granulation method and nature of pore former on anode microstructure. These authors showed porosity as high as 49.1% for a Ni–YSZ substrate prepared by spray drying and containing plate-shaped graphite particles with 5 μm in diameter as pore former. Pratihar et al. [32] reported the preparation of Ni–YSZ cermets by coating YSZ particles with metallic nickel using an electroless coating technique. According to these authors, the electrical conductivity increased with the matrix density for all compositions. This is expected taking into consideration better Ni-to-Ni contact as a result of the decrease in porosity. Even though electrodes with 35% and 44% porosity have shown close conductivity values, authors claim that the suitability of these materials for SOFC application cannot be guaranteed until further work to demonstrate their electrochemical performance and stability is carried out.

Since porosity cannot be increased to a very high level due to deleterious effects on the mechanical strength and electrical conductivity [33], the porosity found herein for the 1CGONi-0 sample (lower value among one step anodes), does not qualify it to act as a anode functional layer, but only as a ceramic substrate in anode supported solid oxide fuel cells. Since all reduced samples showed porosities above 20%, mass transfer limitations are expectedly small in the cermets prepared by both synthesis methods [34].

For cermets prepared by two-step synthesis (2CGONi-*x*), only the sample 2CGONi-0 showed low porosity, around 25%. However, after the addition of 10 wt% citric acid, the cermet 2CGONi-10 approached the 35% porosity value indicated for easy diffusion of fuel and reactants [35,36].

SEM micrographs for 1CGONi-0 and 2CGONi-10 cermet anodes are shown in Fig. 3. The high value of open porosity (49%) found for the one-step anode without pore former (Fig. 3a) can be confirmed by the large amount of uniformly distributed pores. The observed microstructural features suggest large triple phase boundaries, thus potentially improving the electrochemical performance of the anode. On the contrary, the microstructure of sample 2CGONi-10 (Fig. 3b) depicted less uniform porosity.

Figs. 3 and 4, the latter obtained under (BSE) back scattered mode, provide a global view of both types of anode precursors. Due to the large presence of well connected submicrometric grains of Ni–Ni and CGO–CGO, it is not possible to resolve Ni and CGO phases using such a SEM magnification. However, this lack of resolution also implies that both phases are indeed clearly submicrometric and intimately dispersed throughout the composite.

Fig. 4 also shows macropores in both cases after 10 wt% additions of pore former, which denotes significant agglomeration of the citric acid in the initial mixture. This is not surprising considering that 10 wt% of pore former corresponds roughly to about 45 vol%, well above the percolation threshold. The fairly homogeneous pore size and distribution obtained for the composites with 5 wt% citric acid (about 27 vol%) confirms the capability of the one-step powders to accommodate a large amount of pore forming agents without compromising the microstructure.

A few small cracks were observed in the 2CGONi-*x* cermets (Fig. 4), whereas the one-step cermets were mostly crack free, even for the highest content of pore former. Microscopic analysis associated with open porosity measurements indicated that additions in excess of 10 wt% pore former in the one-step anode and 20 wt% in the two-step anode originated poor microstructures which can have a deleterious effect on the anode structural performance. In addition to the

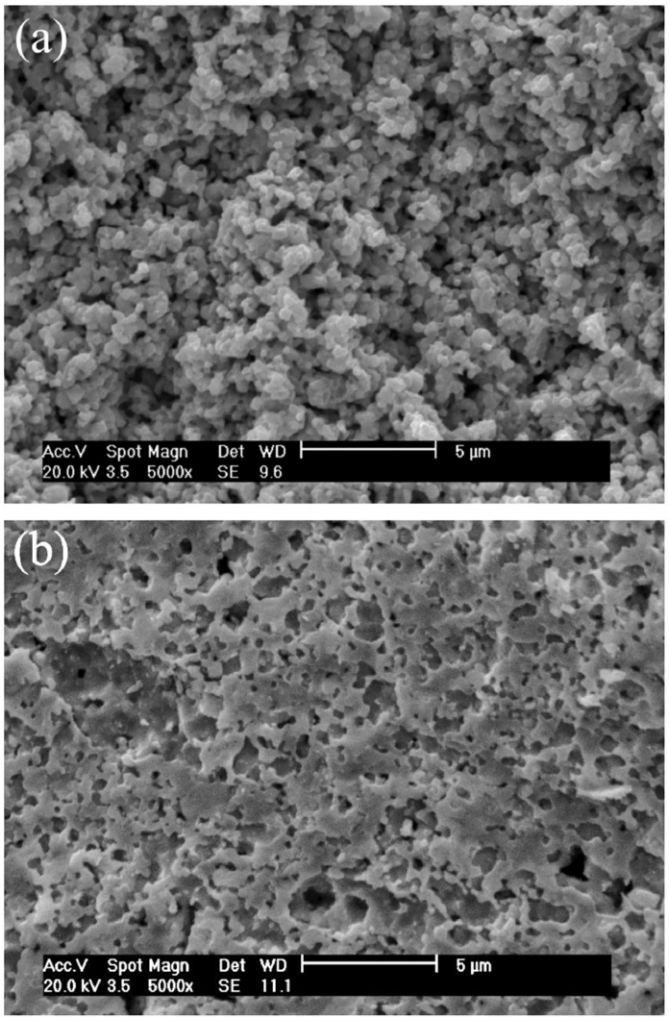

Fig. 3. SEM micrographs of Ni–CGO cermet anodes. (a) 1CGONi-0 (49% porosity) and (b) 2CGONi-10 (36% porosity).

aforementioned highly uniform distribution of pores, it is also clear that better phase dispersion took place in one-step cermets. Nevertheless, phase agglomeration at a micrometric scale is clearly visible in the microstructure of two-step 2CGONi-*x* cermets.

Since the final properties of the Ni–CGO anode are strongly dependent on the precursor composite NiO–CGO, it is of great interest to investigate these materials prior to NiO reduction. Therefore, the electrical characterization of selected NiO–CGO samples was carried out between 90 and 260 °C by impedance spectroscopy, temperature range selected by the quality of the information obtained in these circumstances. Fig. 5 shows the impedance spectra for two selected samples, 1NiOCGO-0 and 2NiOCGO-10, measured before NiO reduction, in air at 200 °C. Two overlapping semicircles are clearly observed comprising the whole frequency range studied, in good agreement with previously reported results [24]. The high and low frequency arcs resemble grain and grain boundary contributions, respectively, but the actual composite response is by far more complex than for a simple polycrystalline ceramic electrolyte, as this description suggests. In fact, both solid phases provide continuous pathways for charge transport, with CGO providing the ionic pathway while NiO provides one electronic pathway. However, it can be shown that one electronic pathway parallel to the ionic pathway is only responsible for a shift in the magnitude of the observed impedance arcs with respect to those expected for the single electrolyte phase. This can be easily modeled as previously suggested in the literature [37]. In such circumstances, the observed characteristics of impedance arcs (hereby named grain and grain boundary) correspond to a blended performance of ionic and electronic transport, although impedance spectra might preserve the shape typical of polycrystalline solid electrolytes.

Furthermore, the presence of significant porosity in these composites, not only acting as a simple insulator but also originating local constriction resistances to charge transport, might also influence the shape of impedance spectra in a complex manner [38]. Nevertheless, and irrespective of the limited physical meaning of this procedure, all impedance data were fitted using the nonlinear least squares fitting program of the Z-view software, and this simplified description of grain and grain boundary contributions.

Grain (σ_g) and grain boundary (σ_{gb}) conductivities for both one-step and two-step composites, as a function of operating temperature, are shown in Fig. 6. As it can be observed, the value of σ_g exceeds σ_{gb} for both types of precursor anode materials, contrary to the result reported for NiO–CGO composites derived from powders synthesized by a ceramic route [24]. Since the ionic conduction in ceramics is thermally activated, the activation energies (E_a) for grain and grain boundary conduction processes may be calculated by taking into account the usual Arrhenius equation:

$$\sigma = \frac{A}{T}\exp\left(\frac{-E_a}{kT}\right) \quad (1)$$

where A is the pre-exponential factor, T is the absolute temperature, and k is the Boltzmann constant. Obviously, considering previous comments, the parameters estimated in this manner are not representative of the intrinsic properties of the electrolyte phase but, instead, include a contribution due to the presence of parallel electronic conduction by NiO, maybe also some influence of porosity.

The calculated activation energies were found to be in the range 0.43–0.44 eV for grain conductivity and 0.39 eV for grain boundary conductivity. These values, not even reaching 0.5 eV, are well below those characteristics of CGO, but coherent in magnitude with those reported elsewhere [25] for NiO–CGO composites with 60 mol% NiO. Consistently, all samples under investigation in the present study were prepared with 70 mol% NiO (50 wt% NiO). Also, the activation energy is expected to portrait the complex composite characteristics of NiO–CGO samples.

Total electrical conductivities of 8.5×10^{-3} Scm^{-1} and 7.1×10^{-3} Scm^{-1} were obtained at 260 °C for the samples

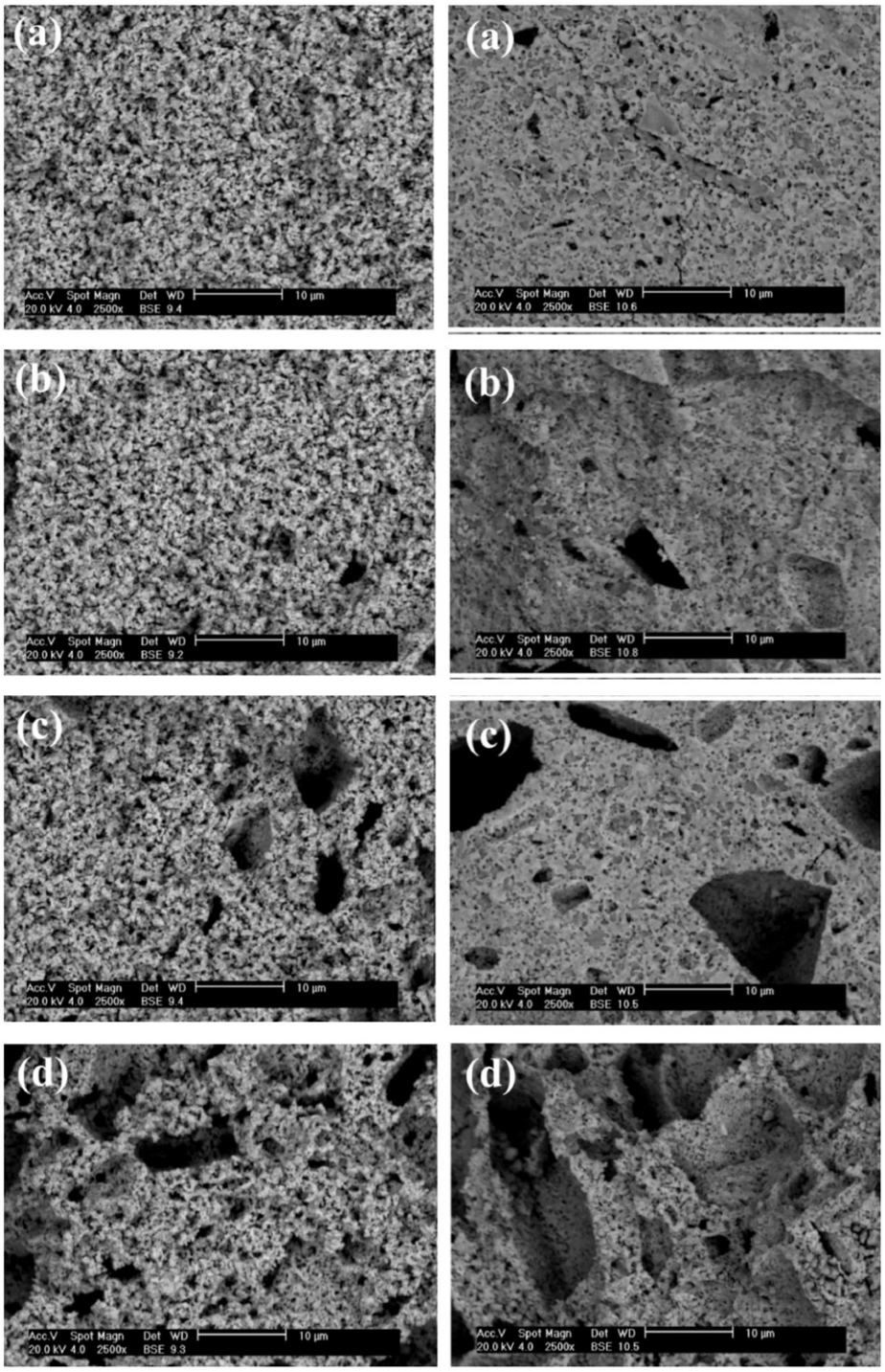

Fig. 4. BSE images of (left) 1CGONi-x and (right) 2CGONi-x cermet anodes with (a) 0, (b) 5, (c) 10 and (d) 20 wt% of pore forming agent.

derived from one-step (1NiOCGO-0) and two-step (2NiO-CGO-10) synthesis, respectively. Since both composites have the same chemical composition, the slightly better electrical response achieved from one-step route was associated with the presence of a network of well-connected and homogeneously distributed NiO and CGO grains in the one-step composite, ensuring better transport of charge carriers. In fact, the total conductivity of these composites exceeds the usual values measured for CGO (lower than 10^{-3} Scm^{-1} at temperatures below 300 °C), which can only be explained by the higher conductivity of the NiO phase acting as a parallel pathway for charge transport. Also, given the widespread range of values (more than five orders of magnitude) reported for the conductivity of NiO [39], due to the enormous influence of non-stoichiometry and minor impurities on the defect concentration and transport properties of NiO, any attempt to further model the conductivity of these composites would be doubtful.

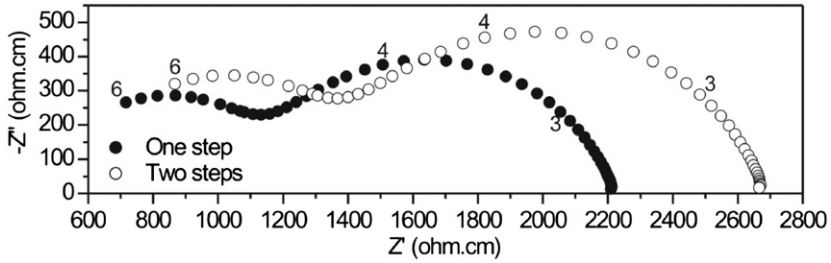

Fig. 5. Impedance spectra of selected one- (1NiOCGO-0) and two-steps (2NiOCGO-10) composites, recorded in air at 200 °C. The numbers correspond to $\log_{10}$ of the frequency.

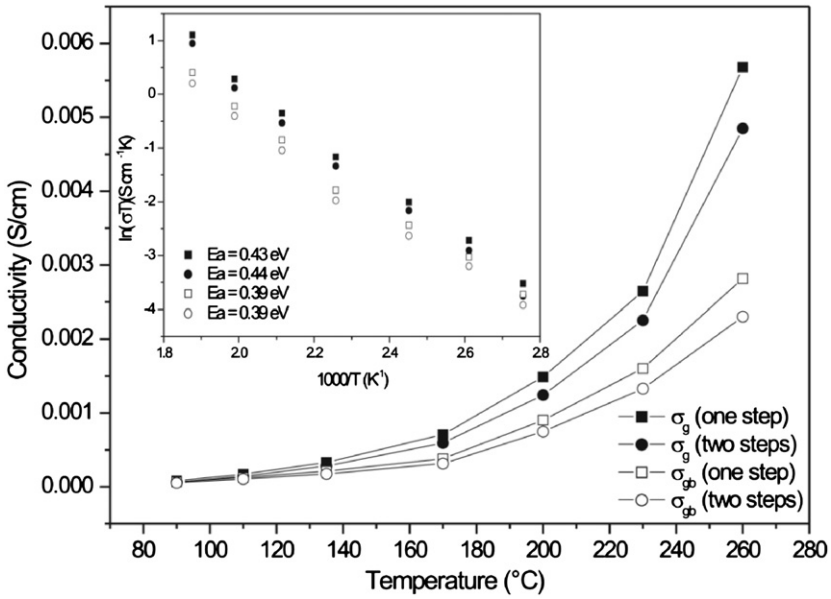

Fig. 6. Temperature dependence of grain (σ_g) and grain boundary (σ_{gb}) conductivity for 1NiOCGO-0 and 2NiOCGO-10 samples. The inset shows the corresponding Arrhenius plots.

Based on combined microstructural and impedance spectroscopy results, and disregarding the considerable difference in the level of porosity, it is possible to infer that the TPB length and the conductivity of one-step cermet anodes must be higher than that of two-steps samples under typical anode operating conditions. The findings in this study indicate the potential of the one-step processing route to develop anodes for low/intermediate-temperature SOFCs. Further investigation is expected to compare the mechanical and electrical properties of one- and two- step Ni–CGO cermets, as a function of the anode sintering temperature, in order to identify optimum fabrication conditions for the best performance of anode-supported SOFCs.

4. Conclusions

The effects of processing route and citric acid content, used as pore forming agent, on the porosity, electrical properties and microstructure of Ni(or NiO)–CGO cermets (or composites) obtained by one- and two-step synthesis was successfully investigated. From X-ray powder diffraction data it is possible to conclude that one-step synthesis results in ultrafine NiO particles and homogeneous nanocrystallites for both NiO and CGO phases. Results indicate that, regardless the powder preparation method, the amount of pore former had a strong influence on the microstructure of the cermets. A remarkable advantage of the one-step synthetic route is its additional flexibility with respect to processing conditions towards the manufacture of Ni–CGO cermets with variable level of porosity, especially suitable for multilayered anode-supported assemblies. The high electrical conductivity obtained for the one-step composite due to the formation of a network of well-connected and homogeneously distributed fine grains, is appropriate to ensure percolation and easy transport of charge carriers. The findings in this work indicate that the in situ nanocomposite NiO–CGO powders are potential candidates to be used as anode component in low/intermediate-temperature SOFCs.

Acknowledgments

The authors acknowledge PPGCEM-UFRN, CAPES (PRÓ-ENGENHARIAS and PDEE program – BEX 6775/10-1), and FCT (Portugal) for their financial support.

References

[1] P.I. Cowin, C.T.G. Petit, R. Lan, J.T.S. Irvine, S. Tao, Recent progress in the development of anode materials for solid oxide fuel cells, Advanced Energy Materials 1 (2011) 314–332.

[2] W.Z. Zhu, S.C. Deevi, A review on the status of anode materials for solid oxide fuel cells, Materials Science and Engineering A 362 (2003) 228–239.

[3] S.P. Jiang, S.H. Chan, A review of anode materials development in solid oxide fuel cells, Journal of Materials Science 39 (2004) 4405–4439.

[4] I. Kang, Y. Kang, S. Yoon, G. Bae, J. Bae, The operating characteristics of solid oxide fuel cells driven by diesel autothermal reformate, International Journal of Hydrogen Energy 33 (2008) 6298–6307.

[5] L. Holzer, B. Münch, B. Iwanschitz, M. Cantoni, T. Hocker, T. Graule, Quantitative relationships between composition, particle size, triple phase boundary length and surface area in nickel-cermet anodes for Solid Oxide Fuel Cells, Journal of Power Sources 196 (2011) 7076–7089.

[6] S.P. Jiang, P.J. Callus, S.P.S. Badwal, Fabrication and performance of Ni/3 mol% Y_2O_3–ZrO_2 cermet anodes for solid oxide fuel cells, Solid State Ionics 132 (2000) 1–14.

[7] S. Murakami, Y. Akiyama, N. Ishida, T. Yasuo, T. Saito, and N. Furukawa, Development of a solid oxide fuel cell with composite anodes, in: F. Grosz, P. Zegers, S.C. Singhal, O. Yamamoto (Eds.), Proceedings of the Second International Symposium on Solid Oxide Fuel Cells (SOFC II), Athens, 1991, pp. 105–112105–112105–112.

[8] X. Deng, A. Petric, Geometrical modeling of the triple-phase-boundary in solid oxide fuel cells, Journal of Power Sources 140 (2005) 297–303.

[9] V.M. Janardhanan, V. Heuveline, O. Deutschmann, Three-phase boundary length in solid-oxide fuel cells: a mathematical model, Journal of Power Sources 178 (2008) 368–372.

[10] T. Ishihara, T. Shibayama, H. Nishiguchi, Y. Takita, Nickel–Gd-doped CeO_2 cermet anode for intermediate temperature operating solid oxide fuel cells using $LaGaO_3$-based perovskite electrolyte, Solid State Ionics 132 (2000) 209–216.

[11] C. Ding, H. Lin, K. Sato, T. Hashida, Synthesis of NiO–$Ce_{0.9}Gd_{0.1}O_{1.95}$ nanocomposite powders for low-temperature solid oxide fuel cell anodes by co-precipitation, Scripta Materialia 60 (2009) 254–256.

[12] B. Rösch, H. Tu, A.O. Stormer, A.C. Müller, U. Stimming, Electrochemical characterization of Ni-$Ce_{0.9}Gd_{0.1}O_{2-\delta}$ for SOFC anodes, Solid State Ionics 175 (2004) 113–117.

[13] T. Suzuki, Y. Funahashi, T. Yamaguchi, Y. Fujishiro, M. Awano, Development of cube-type SOFC stacks using anode-supported tubular cells, Journal of Power Sources 175 (2008) 68–74.

[14] T. Priyatham, R. Bauri, Synthesis and characterization of nanocrystalline Ni–YSZ cermet anode for SOFC, Materials Characterization 61 (2010) 54–58.

[15] G.C. Mather, F.M. Figueiredo, J.R. Jurado, J.R. Frade, Synthesis and characterisation of cermet anodes for SOFCs with a proton-conducting ceramic phase, Solid State Ionics 162–163 (2003) 115–120.

[16] V. Gil, C. Moure, J. Tartaj, Sinterability, microstructures and electrical properties of Ni/Gd-doped ceria cermets used as anode materials for SOFCs, Journal of the European Ceramic Society 27 (2007) 4205–4209.

[17] Y. Li, Y. Xie, J. Gong, Y. Chen, Z. Zhang, Preparation of Ni/YSZ materials for SOFC anodes by buffer-solution method, Materials Science and Engineering B 86 (2001) 119–122.

[18] B. Cela, D.A. de Macedo, G.L. de Souza, A.E. Martinelli, R.M. do Nascimento, C.A. Paskocimas, NiO–CGO in situ nanocomposite attainment: one step synthesis, Journal of Power Sources 196 (2011) 2539–2544.

[19] S.F. Corbin, P.S. Apté, Engineered porosity via tape casting, lamination and the percolation of pyrolyzable particulates, Journal of the American Ceramic Society 82 (1999) 1693–1701.

[20] J.J. Haslam, A.Q. Pham, B.W. Chung, J.F. DiCarlo, R.S. Glass, Effects of the use of pore formers on performance of an anode supported solid oxide fuel cell, Journal of the American Ceramic Society 88 (2005) 513–518.

[21] R.M.C. Clemmer, S.F. Corbin, Influence of porous composite microstructure on the processing and properties of solid oxide fuel cell anodes, Solid State Ionics 166 (2004) 251–259.

[22] K.F. Chen, Z. Lü, N. Ai, X.Q. Huang, Y.H. Zhang, X.S. Xin, R.B. Zhu, W.H. Su, Development of yttria-stabilized zirconia thin films via slurry spin coating for intermediate-to-low temperature solid oxide fuel cells, Journal of Power Sources 160 (2006) 436–438.

[23] J. Hu, Z. Lü, K. Chen, X. Huang, N. Ai, X. Du, C. Fu, J. Wang, W. Su, Effect of composite pore-former on the fabrication and performance of anode-supported membranes for SOFCs, Journal of Membrane Science 318 (2008) 445–451.

[24] R.V. Wandekar, M. Ali (Basu), B.N. Wani, S.R. Bharadwaj, Physicochemical studies of NiO–GDC composites, Materials Chemistry and Physics 99 (2006) 289–294.

[25] A.U. Chavan, L.D. Jadhav, A.P. Jamale, S.P. Patil, C.H. Bhosale, S.R. Bharadwaj, P.S. Patil, Effect of variation of NiO on properties of NiO/GDC (gadolinium doped ceria) nano-composites, Ceramics International 38 (2012) 3191–3196.

[26] N.T. Yang, X.X. Meng, X.Y. Tan, Z.M. Li, Journal of Inorganic Materials 21 (2006) 409–414.

[27] R.A. Young, A.C. Larson, C.O. Paiva-Santos, User's guide to program DBWS-9807A for Rietveld analysis of X-ray and neutron powder diffraction patterns with a PC and various other computers. School of Physics, Georgia Institute of Technology, Atlanta, GA, USA, 2000.

[28] D.A. Macedo, M.R. Cesário, B. Cela, D.M.A. Melo, C.A. Paskocimas, A.E. Martinelli, R.M. Nascimento, Influence of polymerizing agent on structure and spectroscopic properties of nano-crystalline $La_{0.8}Sr_{0.2}MnO_3$ powders, Crystal Research and Technology 45 (2010) 1166–1170.

[29] R.O. Fuentes, R.T. Baker, Structural, morphological and electrical properties of $Gd_{0.1}Ce_{0.9}O_{1.95}$ prepared by a citrate complexation method, Journal of Power Sources 186 (2009) 268–277.

[30] V. Gil, R. Campana, A. Larrea, R.I. Merino, V.M. Orera, Ni-GDC microtubular cermets, Solid State Ionics 180 (2009) 784–787.

[31] J.H. Lee, J.W. Heo, D.S. Lee, J. Kim, G.H. Kim, H.W. Lee, H.S. Song, J.H. Moon, The impact of anode microstructure on the power generating characteristics of SOFC, Solid State Ionics 158 (2003) 225–232.

[32] S.K. Pratihar, A. Dassharma, H.S. Maiti, Properties of Ni/YSZ porous cermets prepared by electroless coating technique for SOFC anode application, Journal of Materials Science 42 (2007) 7220–7226.

[33] T. Fukui, K. Murata, S. Ohara, H. Abe, M. Naito, K. Nogi, Morphology control of Ni–YSZ cermet anode for lower temperature operation of SOFCs, Journal of Power Sources 125 (2004) 17–21.

[34] M.H. Abbasi, J.W. Evans, I.S. Abramson, Diffusion of gases in porous solids: Monte Carlo simulations in the Knudsen and ordinary diffusion regimes, AIChE Journal 29 (1983) 617–624.

[35] Y.H. Yin, W.Y. Zhu, C.R. Xia, G.Y. Meng, Gel-cast NiO–SDC composites as anodes for solid oxide fuel cells, Journal of Power Sources 132 (2004) 36–41.

[36] S.P.S. Badwal, K. Foger, Solid oxide electrolyte fuel cell review, Ceramics International 22 (1996) 257–265.

[37] E. Gomes, F.M. Figueiredo, F.M.B. Marques, Mixed conduction induced by grain boundary engineering, Journal of the European Ceramic Society 26 (2006) 2991–2997.

[38] M. Kleitz, M.C. Steil, Microstructure blocking effects versus effective medium theories in YSZ, Journal of the European Ceramic Society 17 (1997) 819–829.

[39] F.J. Morin, Electrical properties of NiO, Physical Review 93 (1954) 1199–1204.